The Journal of Neuroscience, January 15, 2002, 22(2):377–388

Modulatory Mechanism of the Endogenous Peptide Catestatin on Neuronal Nicotinic Acetylcholine Receptors and Exocytosis

Carlos J. Herrero,[1] Eva Alés,[1] Antonio J. Pintado,[1] Manuela G. López,[1] Esther García-Palomero,[1] Sushil K. Mahata,[2] Daniel T. O'Connor,[2] Antonio G. García,[1] and Carmen Montiel[1]

[1]Departamento de Farmacología and Instituto Teófilo Hernando, Facultad de Medicina, Universidad Autónoma de Madrid, 28029 Madrid, Spain, and [2]Department of Medicine and Center for Molecular Genetics, University of California at San Diego, San Diego, California 92161

The catestatin fragment of chromogranin A is the first known endogenous compound able to inhibit catecholamine release elicited by the activation of neuronal nicotinic acetylcholine receptors (nAChRs) of different animal species and catecholaminergic cell types. However, how catestatin regulates the receptor activity, which subunit combination of the heteropentameric forms of receptor is better blocked by the peptide, or how it affects the different stages of the exocytotic process have not yet been evaluated. To address these questions, we have assayed the effects of catestatin: (first) on the inward currents elicited by ACh (I_{ACh}) in voltage-clamped oocytes expressing different combinations of nAChR subunits; and (second) on the cytosolic Ca^{2+} concentration, $[Ca^{2+}]_c$, and quantal release of catecholamines simultaneously monitored in single adrenal chromaffin cells stimulated with ACh. Catestatin potently blocks all the subtypes of nAChRs studied. Furthermore, it inhibits the $\alpha_3\beta_4$ current in a reversible, noncompetitive, voltage-, and use-dependent manner, a behavior compatible with open-channel blockade. In fura-2-loaded single chromaffin cells, the peptide reduced the $[Ca^{2+}]_c$ signal and the total release of catecholamines elicited by ACh; however, catestatin did not modify the kinetics or the last step of the exocytotic process. Our results suggest that catestatin might play an autocrine regulatory role in neuroendocrine secretion through its interaction with different native nAChR subtypes; the extent of receptor blockade by the peptide could be acutely regulated by the intensity and duration of the presynaptic stimulus.

Key words: catestatin; chromogranin A; $\alpha_3\beta_4$ nAChRs; α_7 nAChRs; $\alpha_4\beta_2$ nAChRs; $\alpha_3\beta_2$ nAChRs; exocytosis; Xenopus *oocytes; chromaffin cells*

Chromogranin A, the major soluble protein in endocrine and neuronal storage secretory vesicles (Blaschko et al., 1967; Winkler et al., 1986; Huttner et al., 1991), has encountered considerable speculation regarding its physiological role, particularly as a precursor of several biologically active peptides. Clues have emerged about the functions of a few peptides cleaved from the chromogranin A molecule; i.e., relaxation of blood vessels and inhibition of parathyroid hormone release by vasostatin (Aardal and Helle, 1992), inhibition of insulin release by pancreastatin (Tatemoto et al., 1986), and the antibacterial activity of secretolytin and chromacin (Goumon et al., 1996; Strub et al., 1996).

Recently, Mahata et al. (1997) discovered a novel fragment of chromogranin A, termed catestatin (bovine chromogranin $A_{344-364}$), which specifically inhibited nicotine-induced norepinephrine release from both rat PC12 pheochromocytoma cells and primary cultures of bovine chromaffin cells. Several forms of catestatin (bovine, human, rat) showed similar inhibitory activity and high homology in their amino acid sequences (Mahata et al., 1997, 2000). These findings raised the hypothesis that catestatin could serve as a novel autocrine modulator of physiological neuroendocrine secretion in chromaffin cells and neurons, wherever the active fragment could be formed and released *in vivo*. This seems to be the case, as judged by the extensive processing of catestatin from chromogranin A found within chromaffin granules and vesicles of bovine chromaffin cells, rat PC12 cells, and postganglionic sympathetic nerves; furthermore, catestatin could be released from stimulated chromaffin cells by an exocytotic mechanism (Taylor et al., 2000).

Early experiments designed to evaluate the effects of catestatin on [^{3}H]-norepinephrine release were performed in cells stimulated with nicotine for several minutes; thus, such experiments failed to provide a full picture of the mechanism of action of the peptide at the neuronal nicotinic acetylcholine receptor (nAChR) or on the secretory process itself, because of poor time resolution. Additionally, the previous experiments did not provide information concerning the subtype of nAChR preferentially blocked by catestatin. This is an important issue, because at least two different classes of nAChRs, most likely formed by the combination of α_3 and β_4 subunits or α_7 subunits that bind α-bungarotoxin, have been implicated in the control of catecholamine secretion in chromaffin cells (Criado et al., 1992; Campos-Caro et al., 1997; López et al., 1998).

In this framework, we planned this study with catestatin to explore the following: (1) the efficacy of the peptide to block currents generated by ACh in *Xenopus laevis* oocytes expressing

Received May 25, 2001; revised Oct. 26, 2001; accepted Oct. 30, 2001.

This work was funded by grants from Dirección General de Investigación Científica y Técnica (PB98-0090, PM99-0005, and PM99-0006) to C.M. and A.G.G., and Programa de Grupos Estratégicos Comunidad Autónoma de Madrid–Universidad Autónoma Madrid (CAM/UAM) and Fundación Teófilo Hernando (FTH), Spain. The work of D.T.O. and S.K.M. is supported by the U.S. Department of Veterans Affairs and National Institutes of Health. C.J.H. was a fellow of FTH; E.A. is a postdoctoral fellow of Programa Grupos Estratégicos (CAM/UAM); A.J.P. and E.G.P. are fellows of CAM, Spain. We thank Prof. F. Sala for helpful comments on an earlier version of this manuscript. We thank Profs. S. Heinemann and J. Patrick for providing the plasmids containing the coding regions of the rat brain nAChR subunits.

Correspondence should be addressed to Carmen Montiel, Departamento de Farmacología, Facultad de Medicina, Universidad Autónoma de Madrid, C/Arzobispo Morcillo 4, 28029 Madrid, Spain. E-mail: carmen.montiel@uam.es.

different combinations of nAChR subunits, (2) the mechanism of the interaction between catestatin and the expressed nAChR, (3) catestatin cleavage from chromogranin A within chromaffin granules from human pheochromocytoma cells, and (4) the actions of catestatin on $[Ca^{2+}]_c$ and the release of catecholamines, measured simultaneously in single mouse chromaffin cells stimulated with short pulses of ACh.

MATERIALS AND METHODS

Techniques for *in vitro* transcription of cDNAs encoding for the nAChR subunits, oocyte injections, and electrophysiological recordings of the expressed foreign receptors, using a virtual ground circuit, have been described previously (Miledi et al., 1989; López et al., 1998; Herrero et al., 1999; Pintado et al., 2000).

Preparation of cRNA and oocyte injection. The plasmids containing the cDNA clones encoding for the α_3, α_4, β_4, β_2, and α_7 rat neuronal nAChR subunits were linearized with the corresponding restriction enzyme and transcribed using the mCAP RNA capping Kit (Stratagene, La Jolla, CA). Mature female *Xenopus laevis* frogs obtained from a commercial supplier (Centre de Recherches de Biochimie Macromoléculaire du Centre National de la Recherche Scientifique, Montpellier, France) were anesthetized with a tricaine solution (0.125%), and ovarian lobes were dissected out. Then, follicle-enclosed oocytes were manually stripped from the ovary membranes and incubated overnight at 16°C in a modified Barth's solution containing (in mM): NaCl 88, KCl 1, $NaHCO_3$ 2.4, $MgSO_4$ 0.82, $Ca(NO_3)_2$ 0.33, $CaCl_2$ 0.41, HEPES 10, buffered to pH 7.4 and supplemented with gentamycin (0.1 mg/ml) and sodium pyruvate (5 mM). The next day, healthy follicle-enclosed oocytes were injected with 50 nl (50 ng) of α_7 RNA or 50 nl (25:25 ng) of α_3/β_4, α_3/β_2, or α_4/β_2 cRNAs, using a Nanoject automatic injector (Drummond Scientific Co., Broomall, PA). Electrophysiological recordings were performed 2–5 d after RNA injections.

Electrophysiology. Experiments with oocytes were performed at room temperature (22–25°C) in Ringer's solution containing (in mM): NaCl 115, KCl 2, $CaCl_2$ 1.8, HEPES 5, buffered to pH 7.4 with NaOH. Inward currents through the nAChRs expressed were recorded with a two-electrode voltage-clamp amplifier (OC-725-B Warner Instrument Corporation, Hamden, CT) using microelectrodes with resistances of 0.5–5 MΩ made from borosilicate glass (GC100TF-15, Clark Electromedical, Pangbourne, UK) and filled with KCl (3 M). The holding potential in all experiments was −60 mV, except in those designed to study the voltage dependence. Single oocytes were held in a 0.3 ml volume chamber and constantly superfused with Ringer's solution by gravity (4 ml/min). The volume in the chamber was maintained constant using the reverse suction of an air pump. Solutions containing ACh or catestatin were applied by means of a set of 2-mm-diameter glass tubes located close to the oocyte. Voltage protocols, ACh pulses, and data acquisition were controlled using a Digidata 1200 Interface and the CLAMPEX software (Axon Instruments, Foster City, CA).

Flash photolysis of Ca^{2+} from a caged-Ca^{2+} compound injected into the oocytes. These experiments, designed to directly activate the native Ca^{2+}-activated chloride current ($I_{Cl(Ca)}$) expressed in oocytes, were performed as described previously (Montiel et al., 1997; Pintado et al., 2000). Briefly, oocytes were injected with 41 nl of the caged-Ca^{2+} solution containing 50 mM DM-nitrophen, 45 mM $CaCl_2$, 5 mM HEPES, at pH 7. After equilibrium in the dark for at least 30 min, individual oocytes were voltage clamped at −60 mV. $I_{Cl(Ca)}$ was activated by Ca^{2+} released from the caged-Ca^{2+} compound after the application of repetitive flashes of light using a high intensity Xenon flash lamp system (Cairn Research Ltd., Faversham, Kent, UK). Ultraviolet light was focused onto the oocyte surface using a light guide positioned over the vegetal pole. The capacitance value used was 2000 μF charged to 200 V. Repetitive flashes of constant intensity and duration were given to the oocyte every 4 min; flashes were controlled by a PC computer using the CLAMPEX software. Under these experimental conditions, caged-Ca^{2+}-injected oocytes gave reproducible $I_{Cl(Ca)}$ responses after repetitive flashes.

Mass spectrometric analysis of immunoprecipitated catestatin from chromaffin granules. Chromaffin granules from freshly obtained human pheochromocytoma were prepared by centrifugation on 0.3 M/1.6 M sucrose density step gradients, lysed in 1 mM NaH_2PO_4 at pH 6.5, and centrifuged to remove granule membranes (Mahata el al., 1997). Then, catestatin was immunoprecipitated (IP) from the granule soluble core lysate using a polyclonal rabbit antibody that recognizes the catestatin region of human chromogranin $A_{352–372}$ (SSMKLSFRARAYGFRGPGPQL), according to the protocol described by Taylor et al. (2000). After immunoprecipitation and washing of the IP product, immunoprecipitated catestatin was subjected to matrix-assisted laser desorption ionization (MALDI) mass spectrometry using a Voyager-Elite mass spectrometer. Samples were embedded in an α-cyano-4-hydroxycinnamic acid matrix and then irradiated with a nitrogen laser at 337 nm, and the ions produced were accelerated with a deflection potential of 30,000 V. Ions were then differentiated according to their mass/charge ratio (m/z) using a time-of-flight mass analyzer. The mass error of this method is characteristically ≤0.1%. Molecular weights from MALDI mass spectra were interpreted, and peptide fragments within the chromogranin A primary structure were assigned by the program PAWS (Protein Analysis WorkSheet, version 8.1.1., for Macintosh), assigning average isotopic MH^+ values for chromogranin A peptides as described previously (Taylor et al., 2000).

Simultaneous electrochemical detection of $[Ca^{2+}]_c$ and catecholamine release from single mouse chromaffin cells. Cells were isolated and cultured as described previously (Hernández-Guijo et al., 1998). Recordings were made on days 2–5 in culture. Cells attached to glass coverslips were loaded with the acetoxy-methyl ester form of the fluorescent dye fura-2 (fura-2 AM) (2.5 μM for 40 min at 37°C, in the dark). Then, cells were washed with Krebs'–HEPES solution (in mM: NaCl 144, KCl 5.9, $MgCl_2$ 1.2, $CaCl_2$ 2, HEPES 10, glucose 11; pH 7.3, titrated with NaOH) and kept for 10 min at 37°C in an incubator before being placed in a perfusion chamber mounted on the stage of a Nikon Diaphot inverted microscope. The chamber was perfused continuously, at room temperature, with Krebs'–HEPES. Solutions containing ACh and/or catestatin were changed using a multibarreled concentration-clamp device (Gandía et al., 1993). Only one experimental protocol was run on each single coverslip. Microelectrodes for the detection of catecholamine release were prepared by introducing a carbon-fiber electrode (12 mm radius) into a patch pipette (Portex, Kent, UK), insulated as described (Chow et al., 1992), and sealed into glass micropipettes with epoxy (CIBA-Geigy). Microelectrodes (20–60 GΩ) were backfilled with 3 M KCl solution and connected to a homemade amplifier. A constant voltage of 780 mV versus Ag/AgCl reference was applied to the electrode. The tip of the carbon-fiber electrode was gently pressed against the cell surface. The amperometric current was filtered at 2 kHz and sampled at 1 kHz. Single-cell fluorescence measurements were performed by exciting the fura-2-loaded cells with alternating 360 and 390 nm filtered light. The apparent $[Ca^{2+}]_c$ was calculated from the ratio of the fluorescence signal (Grynkiewicz et al., 1985): $[Ca^{2+}]_c = K_{eff}(R - R_0)/(R_1 - R)$, where K_{eff} is an "effective binding constant," R_0 is the fluorescence ratio at zero Ca^{2+}, and R_1 is the limiting ratio at high Ca^{2+}. These calibration constants were experimentally determined as described previously (Almers and Neher, 1985). R is the observed or experimental ratio. An ADInstrument MacLab/4e interface controlled by a Macintosh G4 running the MacLab Chart application was used to record, display, and analyze simultaneously the $[Ca^{2+}]_c$ and electrochemical data. Individual spike characteristics were analyzed using the automatic analysis program IGOR (Wavemetrics, Lake Oswego, OR) and the macros described by Segura et al. (2000).

Materials and solutions. If not specified, all products were purchased from Sigma (Madrid, Spain). DMEM, fetal calf serum, and antibiotics were obtained from Invitrogen (Madrid, Spain). Fura-2 AM was from Molecular Probes (Leiden, The Netherlands). Catestatin (bovine chromogranin A derivative peptide A (RSMRLSFRARGYGFRGPGLQL) was synthesized according to Mahata et al. (1997).

Fitting procedure and statistical analysis. Values of agonist concentration eliciting half-maximal current (EC_{50}), antagonist concentration eliciting 50% blockade of maximal current (IC_{50}), and Hill coefficient (n_H) were estimated through nonlinear regression analysis using the four-parameter logistic equation of the GraphPad Prism software for a PC computer. To calculate the time constants (τ) for blockade and recovery of the nicotinic responses, records were fitted to a single exponential curve. Results are expressed as means ± SE. Differences between groups were compared by Student's t test using the statistical program Statworks; a value of $p \leq 0.05$ was taken as the limit of statistical significance.

RESULTS

Catestatin causes fast and reversible blockade of ACh-evoked currents

Oocytes expressing $\alpha_3\beta_4$ nAChRs generated large inward currents (I_{ACh}) after application of ACh onto their surface. An

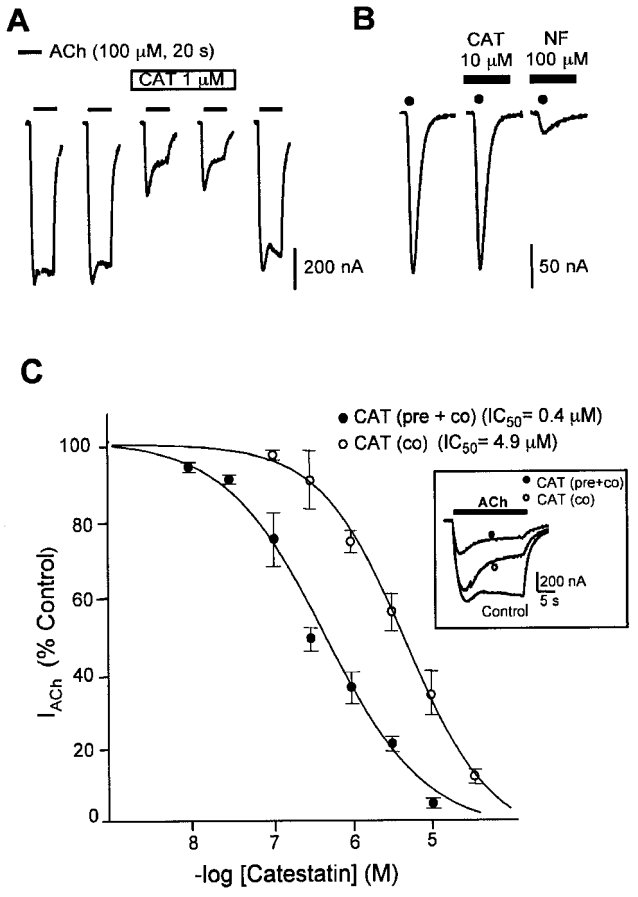

Figure 1. Catestatin reduces $\alpha_3\beta_4$ current (I_{ACh}) expressed in oocytes, with different potencies according to its mode of application. *A*, Typical oocyte expressing $\alpha_3\beta_4$ nAChRs, voltage clamped at −60 mV, and continuously superfused with Ringer's solution. Successive pulses of ACh (100 μM, 20 sec) were applied every 2 min, as shown by the *top horizontal black bars*. After 2–3 initial ACh pulses, this protocol gives reproducible signals for >12 pulses. When I_{ACh} is stabilized, catestatin (*CAT*) was added 1 min before and during the next two ACh pulses, as indicated by the *white horizontal bar*. *B*, Native Ca^{2+}-activated chloride currents, $I_{Cl(Ca)}$, recruited by Ca^{2+} photoreleased from a caged-Ca^{2+} compound previously injected into a typical oocyte. Three light flashes, applied 4 min apart, were used to induce the photorelease (as indicated by the ●). Catestatin (*CAT*) or niflumic acid (*NF*), a specific $I_{Cl(Ca)}$ blocker, was applied as indicated by the *top horizontal black bars*. Each trace of $I_{Cl(Ca)}$ represents a period of 700 msec. This experiment was reproduced in three additional oocytes, with similar results. *C*, Concentration–response curves for catestatin blockade on I_{ACh} using two catestatin application protocols. Values were expressed as percentage of control I_{ACh} (in the absence of peptide), measured at the peak amplitude. The first application protocol consisted of the addition of catestatin during the ACh pulse (*co*, coapplication); in the second, catestatin was preincubated 1 min before the ACh pulse and maintained during the pulse (*pre+co*, preincubation plus coapplication). Each *point* represents means ± SE of values obtained in 6–10 oocytes. *C*, *Inset*, Original traces of I_{ACh} obtained from one oocyte stimulated with successive ACh pulses (as in *A*), in the absence (*Control*) or presence of 1 μM catestatin, using the two application protocols. The maximum blockade on I_{ACh} was achieved with the *pre+co* mode.

example of such currents is shown in Figure 1*A*. These original traces were obtained in an oocyte voltage clamped at −60 mV and intermittently stimulated with 20 sec pulses of 100 μM ACh, given at 2 min intervals. Observe that control I_{ACh} peaks had similar amplitudes after repeated stimulation; currents were reproducible for >12 pulses (data not shown). To determine the effects of catestatin on I_{ACh}, the peptide (1 μM) was introduced into the superfusion system, and two successive ACh pulses were applied in its presence; catestatin was added 1 min before the ACh pulse and maintained throughout the next ACh pulse. Catestatin produced a fast blockade of I_{ACh}; the maximum effect on the peak current amplitude (~60% blockade) was already observed during the first ACh pulse. The blocking effect of catestatin was readily reversible after its washout (Fig. 1*A*, *fifth trace* to the *right*).

Because the nAChR ion pore is permeable to Ca^{2+} in addition to Na^+ (Seguela et al., 1993), it was important to rule out that rather than a direct antagonist action of catestatin on the nAChR itself, the effect of the peptide on I_{ACh} might have resulted from a blockade of the current generated by native chloride channels highly expressed in oocytes (Miledi and Parker, 1984). This chloride current, $I_{Cl(Ca)}$, could be activated by Ca^{2+} flowing through the receptor ion channel. The result shown in Figure 1*B* proves that this was not the case. In this experiment, traces of $I_{Cl(Ca)}$ were obtained in one oocyte injected with DM-nitrophen-caged Ca^{2+} (see Materials and Methods). Flashes of light, applied at 4 min intervals, elicited $I_{Cl(Ca)}$ peaks of reproducible amplitude. Catestatin, at the concentration of 10 μM that fully blocks I_{ACh} through $\alpha_3\beta_4$ receptors (Fig. 1*C*), did not affect $I_{Cl(Ca)}$. This result contrasts with the nearly full current blockade caused by 100 μM niflumic acid, a selective blocker of $I_{Cl(Ca)}$.

Concentration-dependent blockade of I_{ACh}, induced by catestatin when applied in two different modes

Two modes of catestatin application were assayed in $\alpha_3\beta_4$-injected oocytes to determine the mechanism of I_{ACh} blockade by the peptide. The experimental procedure consists of successive ACh pulses (100 μM, for 20 sec) applied at regular 2 min intervals. When I_{ACh} responses became stable, after two or three initial ACh control pulses, catestatin (1 μM) was superfused as follows: (first) in the coapplication mode, the peptide was given just during the ACh pulse; (second) in the preincubation plus coapplication mode, catestatin was given 60 sec before as well as during the ACh pulse. Figure 1*C* (*inset*) shows the original traces of I_{ACh} obtained from one oocyte using the two protocols of catestatin applications; the maximum blockade on I_{ACh} (measuring the peak amplitude or the net charge) was achieved with the second application mode. With the two modes of catestatin delivery, the effect of the peptide on I_{ACh} developed gradually along the ACh pulse. The concentration–response curves plotted in Figure 1*C* were obtained from different oocytes, and they represented the blockade of the peak I_{ACh} exerted by increasing concentrations of catestatin, when the peptide was assayed according to the two protocols described above. Values were expressed as percentage of control response evoked by ACh alone (100%). The IC_{50} values for catestatin blockade of I_{ACh} obtained from these curves were 4.9 μM when the peptide was present only during the ACh pulse and 0.4 μM when catestatin was also preincubated. When calculating the net charge values of I_{ACh}, rather than the peak amplitude, the IC_{50} values obtained were 2.1 and 0.2 μM in the absence or presence of catestatin preincubation, respectively; note that differences in blockade between the two modes of peptide delivery were still maintained.

Noncompetitive blockade of I_{ACh} by catestatin

To further study the mechanism whereby catestatin blocks nAChRs, we assayed the effects of the peptide on $\alpha_3\beta_4$ currents elicited by increasing concentrations of ACh, applied as sequen-

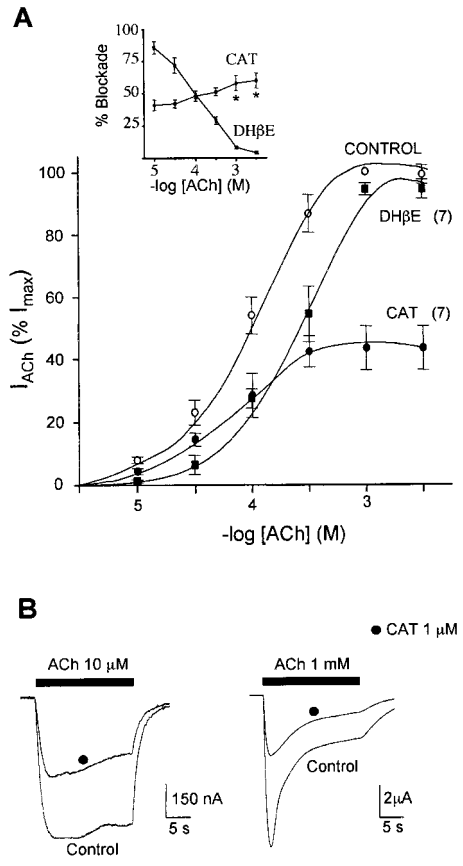

Figure 2. Catestatin blocks $\alpha_3\beta_4$ receptors in a noncompetitive manner. *A*, The concentration–response curve for catestatin (1 μM) and dihydro-β-erythroidine (*DHβE*, 10 μM) on I_{ACh} elicited by sequential pulses of increasing concentrations of ACh (*abscissa*). Each oocyte was stimulated with pulses of increasing concentrations of ACh of 20 sec duration, applied at 2 min intervals. We took advantage of the ready reversibility of catestatin blockade to assay the effects of two to four different concentrations of the peptide in each individual oocyte. Each response was normalized to the response of the same oocyte to 1 mM ACh (100%), a concentration of ACh that elicited the maximal current (I_{max}). Data are means ± SE of values obtained in the number of oocytes shown in *parentheses*. The *inset* represents the relative percentage of blockade of control I_{ACh} exerted by the two blockers, at each concentration of ACh. Blockade of I_{ACh} by catestatin was significantly greater at higher (1 or 3 mM) than at lower ACh concentrations (10 or 30 μM; $^*p < 0.05$). *B*, Original traces of the $\alpha_3\beta_4$ currents elicited by two different concentrations of ACh (10 μM and 1 mM) assayed in the same oocyte, revealing a higher blockade by catestatin of I_{ACh} elicited by 1 mM Ach. Note the different calibration bars.

tial pulses (20 sec) every 2 min, to avoid receptor desensitization. Figure 2*A* shows the control I_{ACh} curve; data points represent the peak amplitude of ACh-evoked currents expressed as percentage of the maximum response to ACh alone (I_{max}), which was reached with 1 mM ACh. The threshold concentration of ACh capable of inducing a measurable current was 10 μM. Figure 2*A* also represents the peak amplitudes of the I_{ACh} curve in the presence of 1 μM catestatin (added 1 min before and during the ACh pulse); data were expressed as percentage of the I_{max} obtained from the same oocyte, in the absence of catestatin. The results from different oocytes were compiled to generate a plot of mean peak current amplitude versus ACh concentration. Note that catestatin blockade was insurmountable by increasing concentrations of ACh; moreover, as shown in Figure 2*A*, *inset*, the peptide reduced by 59 ± 7% the peak current amplitude evoked by 1 mM ACh, whereas blockade was significantly lower when I_{ACh} was elicited by 10 μM ACh (40 ± 4%; $p \leq 0.05$). Figure 2*B* shows two original traces of I_{ACh} obtained in the same $\alpha_3\beta_4$-injected oocyte stimulated by ACh (10 μM or 1 mM), in the absence or presence of 1 μM catestatin; note the higher blockade at the higher ACh concentration. To reinforce the noncompetitive nature of the effect of catestatin on the nicotinic receptor, a similar experimental design was performed with 10 μM dihydro-β-erythroidine (DHβE), a well known competitive blocker at the nAChR. This compound produced a parallel shift to the right of the concentration–response curve for ACh (Fig. 2*A*). In contrast to catestatin, we found that DHβE antagonism on I_{ACh} could be overcome by increasing the ACh concentration (Fig. 2*A*, *inset*).

Maximum peak currents (I_{max}) induced by 1 mM ACh, in the absence or presence of blockers, were obtained from the concentration–response curves for ACh in Figure 2*A*. Results show that DHβE did not modify control I_{max} (3.3 ± 0.3 vs 3.0 ± 0.3 μM; $n = 7$); in contrast, catestatin significantly reduced it (from 8.6 ± 1.4 to 4.1 ± 1.1 μM; $p < 0.001$; $n = 7$). Moreover, the half-stimulatory concentration of ACh (EC_{50} = 94.7 ± 8 μM; $n = 14$ oocytes) was significantly reduced in the presence of catestatin (66 ± 5 μM; $p \leq 0.01$). However, in the presence of DHβE, the calculated EC_{50} value for ACh increased to 290 ± 16 μM ($p \leq 0.01$). The calculated Hill coefficient (n_H) for the control ACh curve was 1.42 ± 0.16, whereas n_H values in the presence of catestatin and DHβE were 1.43 ± 0.34 and 1.34 ± 0.46, respectively.

Blockade of $\alpha_3\beta_4$ currents by catestatin exhibits a pronounced voltage dependence

We assayed the voltage dependence of nAChR blockade by the peptide through its capability to inhibit I_{ACh} at different holding potentials. At the beginning, we used brief ACh pulses (100 μM, 1 sec), applied at 1 min intervals, to generate I_{ACh} at different membrane potentials. Under these experimental conditions, 1 μM catestatin that was superfused continuously onto the surface of the $\alpha_3\beta_4$-injected oocytes (during the ACh pulses and intervals between pulses) reduced the current amplitude more at hyperpolarizing than at depolarizing potentials. Pooled results from 13 oocytes using these experimental conditions revealed that at −100 mV, catestatin blocked I_{ACh} by 57 ± 4% and significantly less at −40 mV (35 ± 4%; $p \leq 0.01$).

Although the voltage dependence of catestatin in blocking I_{ACh} was clearly demonstrated through the experiments described above, we attempted to disclose this property more sharply with another protocol, i.e., using longer periods of ACh pulses. Figure 3*A* shows the I_{ACh} trace obtained in an oocyte expressing $\alpha_3\beta_4$ receptors, voltage clamped at −40 mV. To prevent current desensitization during the prolonged stimulation period (160 sec), a moderate concentration of ACh (10 μM) was used. When the current became stable (40 sec after starting the ACh stimulation), catestatin (0.3 μM) was perfused for 60 sec. The peptide caused a quick relaxation of the current, reaching a plateau at ~52% of the initial current; washout of catestatin restored the current amplitude to near its pre-catestatin value. Figure 3, *B* and *C*, shows the results obtained in the same oocyte using a similar protocol, but this time voltage clamped at −60 or −100 mV, respectively. Note that now catestatin produced a faster and higher relaxation of the current, particularly at more hyperpolarized membrane potential; the removal of the peptide produced a slower and incomplete recovery of the current. Averaged pooled results from five oocytes showed 54 ± 3% current blockade at −40 mV, 73 ± 4% at −60 mV, 83 ± 4% at −80 mV, and 92 ± 3% at −100 mV. The

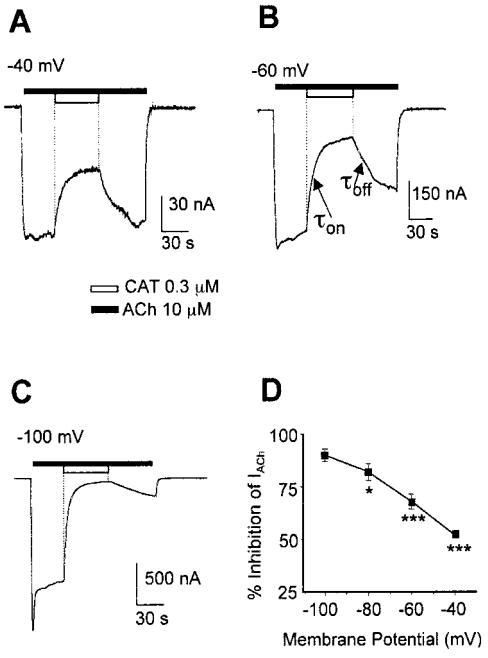

Figure 3. Catestatin exhibits a pronounced voltage dependence in blocking I_{ACh} through $\alpha_3\beta_4$ receptors. *A*, Original trace of the $\alpha_3\beta_4$ current elicited by 3 min application of 10 μM ACh (*top horizontal black bar*) in an oocyte voltage clamped at −40 mV; catestatin was introduced within the ACh pulse, during the period indicated by the *white bar*. *B*, *C*, The original I_{ACh} traces obtained in the same oocyte under similar experimental conditions, but voltage clamped at −60 or −100 mV. *D*, Results of the maximal inhibition of I_{ACh} reached at the end of the catestatin application, at different holding potentials. Data, expressed as percentage of inhibition of peak amplitude before addition of the peptide, are means ± SE of five oocytes. $^*p < 0.05$; $^{***}p < 0.001$; comparing with blockade at −100 mV.

blockade by catestatin of I_{ACh} was fitted to a single exponential at each membrane potential. Values of τ_{on} obtained were 9.8 ± 2.5 sec at −40 mV, 8.8 ± 0.5 sec at −60 mV, and 4.5 ± 0.4 sec at −100 mV; values at −40 mV and −60 mV were significantly different ($p \leq 0.01$) from those obtained at −100 mV. Differences in the time required to remove the blockade after catestatin washout were also found among the different membrane potentials tested. After catestatin was removed, I_{ACh} blockade recovered faster at −40 mV (τ_{off}, 13 ± 5 sec) than at −60 mV (τ_{off} 24 ± 6 sec; $p \leq 0.05$); the blockade at −100 mV was hardly removed.

Blockade by catestatin of I_{ACh} through $\alpha_3\beta_4$ receptors shows use dependence

Two limitations arose while we were planning experiments to define whether the blockade by catestatin of I_{ACh} exhibited use dependence. Thus, repeated stimulation with ACh at short intervals could cause receptor desensitization; additionally, the slow superfusion system precluded the application of very short ACh pulses. Nevertheless, we assayed whether the extent of blockade exerted by catestatin was significantly different using different intervals (5 or 10 sec) between two ACh pulses. Repeated ACh pulsing (100 μM, 0.5 sec; applied every 5 sec) generated currents through $\alpha_3\beta_4$ receptors with peak amplitudes that remained constant for more than 20 consecutive pulses (Fig. 4*A*). Also, when ACh was applied at 10 sec intervals, the current suffered no decay (data not shown). Note in Figure 4*B* that during continuous superfusion of 1 μM catestatin onto an oocyte being stimulated

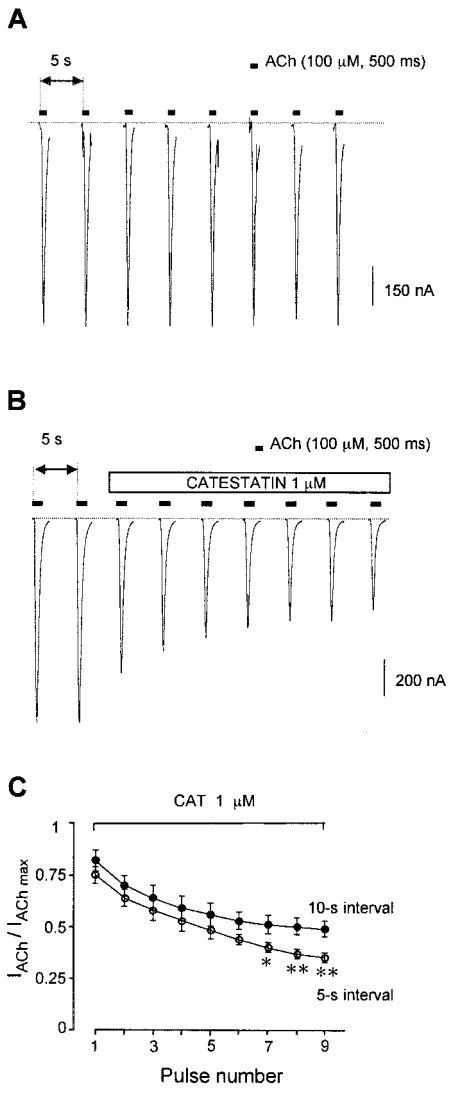

Figure 4. Use-dependent blockade by catestatin of $\alpha_3\beta_4$ currents. *A*, Original I_{ACh} traces obtained in one oocyte expressing $\alpha_3\beta_4$ nAChRs, voltage clamped at −60 mV, and stimulated with repeated brief ACh pulses (100 μM, 500 msec) applied at 5 sec intervals. *B*, Typical $\alpha_3\beta_4$ current traces obtained in one oocyte stimulated initially as above, first in the absence and subsequently in the continuous presence of catestatin, as shown by the *top horizontal bar*. *C*, Pooled results collected from experiments performed in different oocytes, assaying the effect of catestatin on I_{ACh} elicited by repeated ACh pulses applied, first at 5 sec intervals (as above) and subsequently at 10 sec intervals. The initial pre-catestatin I_{ACh} amplitude was normalized to 1 ($I_{ACh\ max}$), and the amplitudes of the currents obtained in the presence of catestatin were expressed in the ordinate as a fraction of the $I_{Ach\ max}$ ($I_{ACh}/I_{ACh\ max}$). Data are means ± SE of eight oocytes from three different donors. $^*p < 0.05$; $^{**}p < 0.01$; comparing the blockade obtained in the same pulse number at the two intervals.

with ACh pulses at 5 sec intervals, the blockade of I_{ACh} developed gradually and become stable after several pulses, at a current amplitude ~36% of the initial I_{ACh}. The current recovered partially after catestatin washout (data not shown). Figure 4*C* shows averaged results of gradual blockade of I_{ACh} caused by 1 μM catestatin, in different oocytes stimulated with successive pulses of ACh, applied at 5 or 10 sec intervals. Note the faster and higher blockade achieved at 5 sec, with respect to 10 sec intervals.

Effects of catestatin on nAChRs composed of different subunit combinations

All experiments described so far were performed on $\alpha_3\beta_4$ nAChRs expressed in oocytes. The reason is that these two subunits are highly expressed in adrenal chromaffin cells (Criado et al., 1992), where catestatin is synthesized, stored, and co-released together with catecholamines (Mahata et al., 1997; Taylor et al., 2000). Furthermore, it has been suggested that nAChRs containing α_3 and β_4 subunits are dominant in the control of catecholamine secretion from these cells (Wilson and Kirshner 1977; Kumakura et al., 1980; Trifaró and Lee, 1980; Kilpatrick et al., 1981). However, bovine chromaffin cells additionally express α_7 nAChRs (García-Guzman et al., 1995), which are also functional (López et al., 1998). Therefore, it was of interest to know whether catestatin blocked nAChR subunit combinations other than the $\alpha_3\beta_4$.

Different combinations of brain nAChR subunits were expressed in oocytes, and to obtain reproducible I_{ACh} for each combination assayed, different periods of ACh pulses and different intervals between successive pulses were selected. Figure 5*A* (*left*) shows I_{ACh} traces obtained after application of 5 sec pulses of 100 μM ACh (applied 2 min apart) onto an oocyte expressing α_7 receptors. The control current relaxed very quickly, likely because of the well established fast desensitization of this receptor subtype after its stimulation with agonists (López et al., 1998; Papke and Thinschmidt, 1998; Herrero et al., 1999). Catestatin (1 μM), added 1 min before and during the ACh pulse, blocked the current by 66%. Figure 5*A* (*middle*) shows a similar experiment performed in an oocyte expressing $\alpha_3\beta_2$ receptors stimulated for 20 sec with pulses of 100 μM ACh (2 min apart). Initially, I_{ACh} through these receptors desensitized quickly and then much more slowly; catestatin (1 μM) blocked by 60% the peak amplitude of the $\alpha_3\beta_2$ current. Finally, Figure 5*A* (*right*) shows the original traces generated by ACh pulses (100 μM, 5 sec) applied at 4 min intervals in an oocyte expressing $\alpha_4\beta_2$ receptors; note that the current also desensitized more slowly than the α_7 current and that 1 μM catestatin blocked this current by 40%. Blockade by catestatin quickly reversed on washout of the peptide, at each of the three receptor types studied (data not shown).

Concentration–response curves for catestatin effects on I_{ACh} were performed in different oocytes expressing α_7, $\alpha_3\beta_2$, or $\alpha_4\beta_2$ nAChRs (Fig. 5*B*). In these experiments, oocytes were stimulated with successive ACh pulses (100 μM) during the period and intervals mentioned above for each receptor type. The IC_{50} values for catestatin blockade were 0.3 μM for α_7, 0.4 μM for $\alpha_3\beta_2$, and 1.7 μM for $\alpha_4\beta_2$ receptors. The calculated EC_{50} value for ACh in oocytes expressing α_7 nAChRs stimulated with increasing concentrations of the agonist, applied as brief pulses (5 sec) every 1 min, was 95 ± 16 μM (n = 10); this EC_{50} value for $\alpha7$ and the EC_{50} *va*lue for $\alpha_3\beta_4$ (98 ± 10 μM) were close to those obtained by Stafford et al. (1994) in oocytes expressing these two receptor subtypes from rat brain. These authors also found that the EC_{50} value for ACh in oocytes expressing rat brain $\alpha_3\beta_2$ and $\alpha_4\beta_2$ nAChRs was 43 μM for both receptor subtypes.

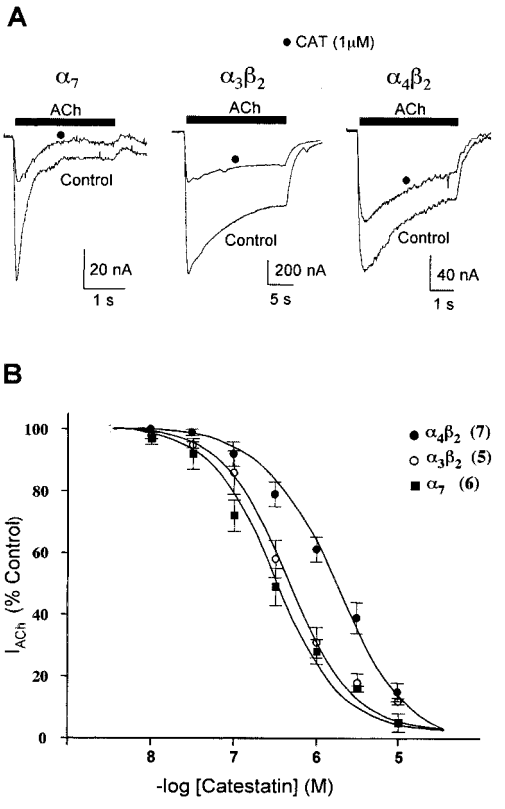

Figure 5. Catestatin potently blocked I_{ACh} generated through α_7, $\alpha_3\beta_2$, and $\alpha_4\beta_2$ nAChRs. These experiments were performed in oocytes expressing different combinations of nAChR subunits, following protocols similar to those described in Figure 2*A*. *A*, Original traces of α_7, $\alpha_3\beta_2$, or $\alpha_4\beta_2$ currents elicited by pulses of ACh (100 μM), in the absence (*Control*) or presence of catestatin (●). For each receptor subtype, different protocols for ACh application were selected to prevent current desensitization: i.e., for α_7 receptors, ACh pulses of 5 sec were applied at 2 min intervals; for $\alpha_3\beta_2$ receptors, ACh pulses of 20 sec were applied at 2 min intervals; and for $\alpha_4\beta_2$ receptors, ACh pulses of 5 sec were applied at 4 min intervals. In all cases, catestatin (*CAT*) was added 1 min before and during the ACh pulse. *B*, Pooled data of the concentration–response curves for the inhibitory effects of catestatin on α_7, $\alpha_3\beta_2$, and $\alpha_4\beta_2$ currents expressed in oocytes. Values represent the amplitude of peak I_{ACh} for each concentration of peptide assayed, and they were normalized in terms of percentage of control I_{ACh} (100%), considered to be the amplitude of peak I_{ACh} preceding the addition of the peptide. Data are means ± SE of the number of oocytes shown in *parentheses*.

Processing of chromogranin A to catestatin in human pheochromocytoma chromaffin granules

Studies of the mechanism of action of catestatin on nAChRs expressed in oocytes have been performed here using the synthetic peptide. However, before studying the modulatory effect of catestatin on a physiological response, such as the exocytotic catecholamine secretion elicited by ACh in chromaffin cells, it is important to show that the catestatin fragment of chromagranin A is indeed formed by endogenous proteolytic cleavage *in vivo*. Our results of MALDI mass spectrometry after anti-catestatin immunoprecipitation of human pheochromocytoma chromaffin granules confirm previous findings indicating that the catestatin fragment of chromogranin A is excised endogenously within the chromaffin granules, at particular amino acid residues (Taylor et al., 2000). The spectrum presented in Figure 6 reveals two peaks. The major peak (at m/z = 3771) corresponds to human chromogranin $A_{340–372}$ (LEGQEEEEDNRDSSMKLSFRARAY-GFRGPGPQL) within the chromogranin A primary structure; calculated m/z (3771) exactly matches with the experimental value obtained. This major form of catestatin is bound on either side by dibasic recognition sites for prohormone cleavage. We also found a smaller quantity of a form with a higher molecular weight (m/z = 5377), compatible with the human chromogranin $A_{353–399}$, which is bound on its C terminus by a dibasic site. Other MALDI

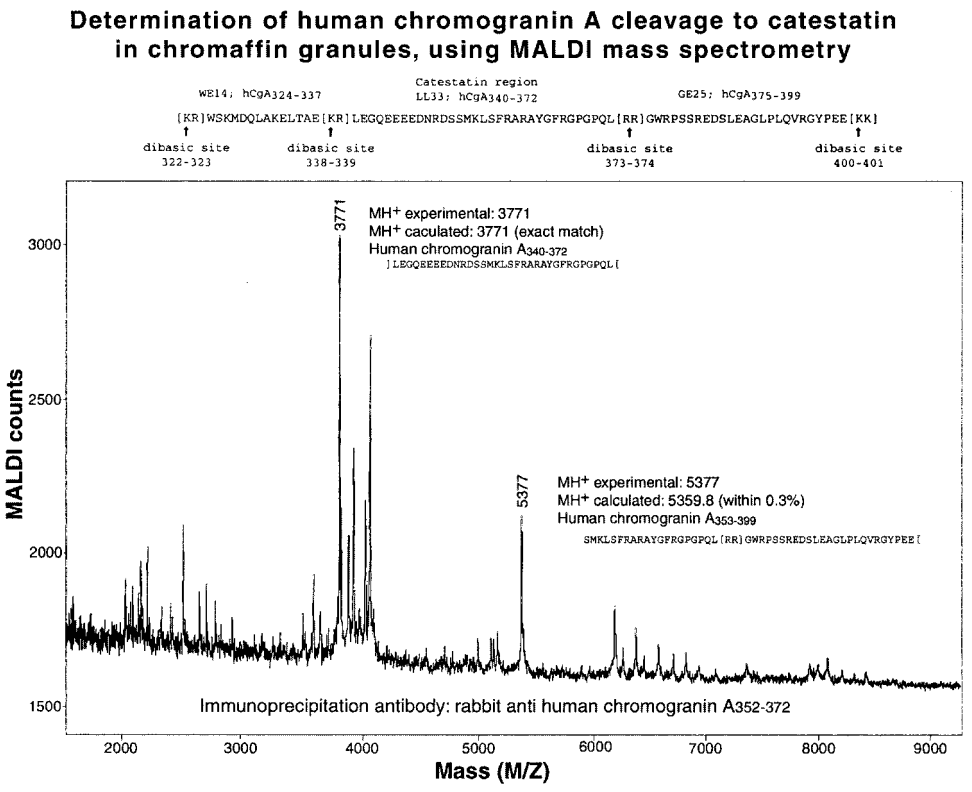

Figure 6. MALDI mass spectrometry identification of catestatin in immunoprecipitated human pheochromocytoma chromaffin granules. Aliquots (200 μl) of pheochromocytoma chromaffin granule soluble core proteins/peptides were immunoprecipitated (20 μl) with rabbit anti-human chromogranin $A_{352–372}$ and then subjected to MALDI mass spectrometry (1–2 μl). A major form of catestatin cleaved at dibasic sites was found (m/z = 3771), as well as a smaller amount of a form containing a C-terminal flanking peptide (m/z = 5377).

peaks in the figure could not be unambiguously assigned within the human chromogranin A primary structure.

Catestatin reduces elevations of $[Ca^{2+}]_c$ and transmitter release evoked by brief ACh pulses in single chromaffin cells

We demonstrated previously that catestatin exerts a clear and selective inhibitory effect on ACh-elicited catecholamine secretion from populations of rat PC12 and bovine chromaffin cells (Mahata et al., 1997). However, in those earlier experiments, the limited time resolution of the protocols used (i.e., [^{3}H]-norepinephrine release from nicotine-stimulated cells and stimulation periods of 15–30 min) could not resolve which particular phase of the exocytotic process mediated by nAChR activation is affected by catestatin. Fura-2 fluorescence measurements combined with the carbon-fiber amperometry records allow simultaneous on-line monitoring of $[Ca^{2+}]_c$ signals and the quantal release of catecholamines in single chromaffin cells. These techniques and experimental conditions keep intact the cytoplasmic constituents of the cell and allow the study of the physiological response induced by brief pulses of ACh. Because robust amperometric responses to ACh are required for analysis of the catestatin effects at the single cell level, we selected the mouse chromaffin cell, which in our hands provides larger and more reproducible signals during repetitive ACh applications. Nonetheless, catestatin also blocked, with similar efficacy, the exocytotic and $[Ca^{2+}]_c$ responses elicited by ACh in single rat and bovine chromaffin cells (experiments not shown).

A brief pulse of ACh (1 mM, 5 sec) applied to single mouse chromaffin cells caused a fast and transient increase of the $[Ca^{2+}]_c$ signal from a resting level of 41 ± 8 nM to 397 ± 65 nM (n = 10). Simultaneously, the evoked electrochemical current (I_{amp}) elicited by ACh correlated well with the $[Ca^{2+}]_c$ signal and exhibited a single secretory component characterized by many superimposed single secretory spikes that are characteristic of quantal release of oxidizable neurotransmitter from single vesicles that fused with the plasma membrane at a high rate while the Ca^{2+} signal persisted (Fig. 7, amperometric traces). Between the first and second $[Ca^{2+}]_c$ or I_{amp} responses induced by the first two pulses of ACh, there is normally a decrease in the signal, but thereafter the responses during subsequent ACh pulses remained stable (see how control responses indicated by *open symbols* in Fig. 8*C*, normalized to the second ACh pulse, are practically constants). For this reason, to calculate the percentage of inhibition induced by catestatin, we took the $[Ca^{2+}]_c$ or I_{amp} signals elicited by the second ACh pulse as 100%. The presence of catestatin (3 μM), added 1 min before and during the ACh pulse, reduced by 30% (286 ± 58 nM) the peak amplitude of the $[Ca^{2+}]_c$ signal (Fig. 7*A*). Consistently, the secretory response expressed as I_{amp} was inhibited proportionally. Moreover, the inhibitory effect on the $[Ca^{2+}]_c$ signal and secretion was partially reversible after washout of the peptide. It is worth noting that when catestatin was present only during the 5 sec of application of the ACh pulse, blockade of the $[Ca^{2+}]_c$ and I_{amp} signals was considerably less (5–10%). The effect of catestatin was specific for the nicotinic receptor-mediated responses, because the peptide did not affect the $[Ca^{2+}]_c$ signal or the amperometric current evoked by cell depolarization (70 mM K^+; data not shown).

Catestatin does not influence the efficacy of $[Ca^{2+}]_c$ to trigger the exocytotic process

Figure 8, *A* and *B*, represents the net values of inhibition of 3 μM catestatin on the global $[Ca^{2+}]_c$ and the total I_{amp} induced by sequential ACh pulses following the protocol described above. These values were calculated by integrating the area under the $[Ca^{2+}]_c$ signal and the amperometric traces obtained in 10 different cells. When both parameters were normalized (referred to as percentage of the response obtained during the second ACh

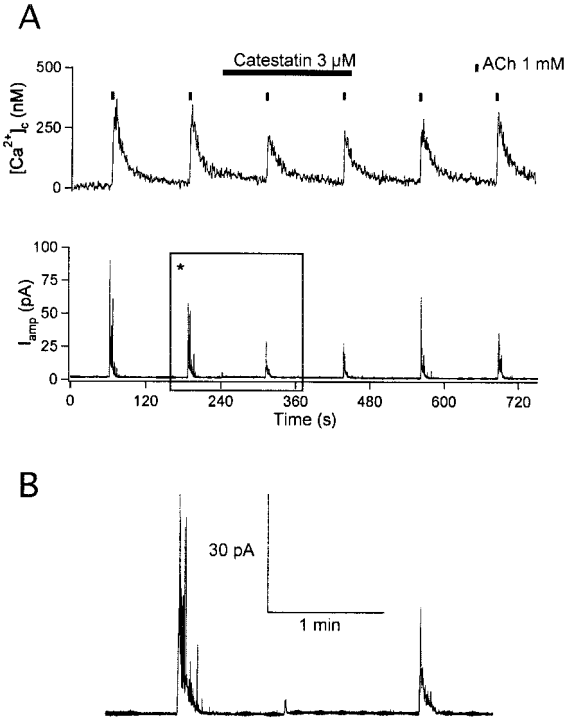

Figure 7. $[Ca^{2+}]_c$ transients and amperometric signals triggered by ACh in the absence and presence of catestatin. *A*, Representative $[Ca^{2+}]_c$ and secretion measured simultaneously in a single mouse chromaffin cell stimulated with six sequential pulses of ACh (1 mM, 5 sec) applied at 2 min intervals. Catestatin was perfused 1 min before the third ACh pulse and maintained throughout until the end of the fourth ACh pulse. *B*, Detail of the exocytotic responses evoked by the second and third ACh pulse in the absence or presence of catestatin, respectively; the difference in the current magnitude is appreciable. In both cases, secretion occurs as an amperometric current burst that reflects exocytosis of catecholamine-containing vesicles at a high rate.

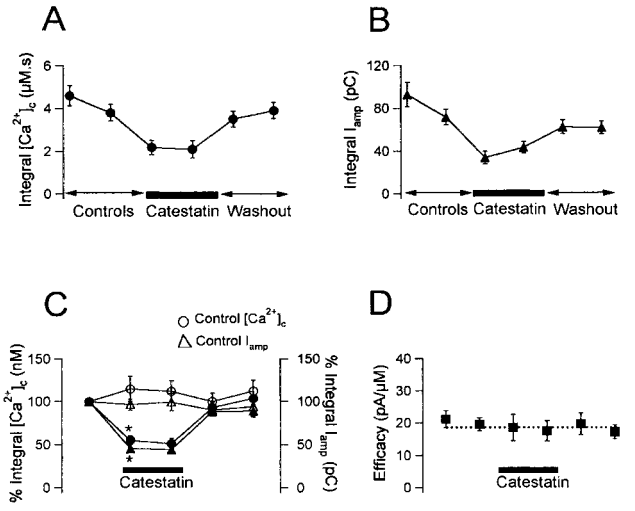

Figure 8. Catestatin diminishes proportionally Ca^{2+} influx and secretion elicited by brief ACh pulses. *A*, *B*, $[Ca^{2+}]_c$ transient integral and amperometric current integral obtained during the stimulation of different single cells with six sequential ACh pulses (1 mM, 5 sec) applied at 2 min intervals; catestatin (3 μM) was added following the protocol identical to that described in Figure 7. Between the first and second ACh pulse, there was normally a decrease in the $[Ca^{2+}]_c$ and in the exocytotic signal, but thereafter the responses elicited by successive ACh pulses remained practically constant, as shown in the control normalized data of *C* (*open symbols*); values are expressed as percentage of the signal elicited by the second ACh pulse (100%). *Filled symbols* represent normalized $[Ca^{2+}]_c$ and secretion values obtained in cells stimulated with ACh as above, but in the presence of catestatin (added where indicated by the *black bar*). The peptide decreased significantly both signals by 45 and 55%, respectively ($^*p < 0.01$). *D*, Efficacy of Ca^{2+} influx to stimulate exocytosis. Values were obtained from the ratio between the amperometric current integral and the $[Ca^{2+}]_c$ integral for each ACh pulse. Values are means ± SE of results obtained in 10 different single cells.

pulse) and compared with their respective control values (obtained in cells stimulated with similar sequential ACh pulses, but in the absence of catestatin), it was observed that the effect of catestatin on the release of catecholamines was proportional to its effect on the global $[Ca^{2+}]_c$ signal (Fig. 8*C*). Thus, the reduction of the $[Ca^{2+}]_c$ integral in the presence of catestatin achieves a proportional reduction of catecholamine secretion. Under control conditions, in the absence of catestatin, the efficacy of exocytosis elicited by ACh, defined as the global catecholamine release per increment in $[Ca^{2+}]_c$, was 18.9 ± 0.61 pA/μM. In the presence of catestatin, this value was not significantly modified from the control (Fig. 8*D*).

Effects of catestatin on kinetics of $[Ca^{2+}]_c$ and exocytotic responses

To understand how catestatin affects kinetic components of the $[Ca^{2+}]_c$ and secretory responses, we measured the global $[Ca^{2+}]_c$ increment and the cumulative charge of amperometric spikes elicited by longer periods of ACh application. Results obtained in a typical cell are shown in Figure 9*A*; the cell was stimulated with two ACh pulses (1 mM, 30 sec), 2 min apart, in the absence (first pulse, control) or presence of 3 μM catestatin added just during the second ACh reintroduction. Results obtained in these experiments reveal that the $[Ca^{2+}]_c$ and the amperometric current elicited by the neurotransmitter persisted even longer than the duration of the ACh pulse. Moreover, the secretory pattern consisted of a first rapid phase, similar to that observed with brief ACh pulses, followed by a second slower-rate secretion phase, in which individual spikes could be distinguished easily (9*A*, *inset*). The presence of catestatin during the second ACh pulse modified substantially the amplitude and accelerated the decay of the $[Ca^{2+}]_c$ signal, which was not modified in the absence of the peptide (data not shown). Averaged curves of the global $[Ca^{2+}]_c$ decay from four different cells stimulated as in Figure 9*A* are shown in Figure 9*B*. Control (ACh alone) and experimental (ACh plus catestatin) decay curves could be fitted to single exponential; catestatin increased by 1.25 times the rate of the $[Ca^{2+}]_c$ decay (τ = 11.3 vs 14.2 sec in the control curve).

The kinetic components of the secretory response were analyzed measuring the accumulated charge of amperometric spikes in chromaffin cells stimulated with ACh, in the absence (control) or presence of catestatin, using a protocol similar to that described in Figure 9*A*. Results in Figure 9*C* (*left*) show the averaged cumulative integral obtained from several cells. Continuous secretion induced by ACh, in the presence of catestatin, showed a marked reduction of the amplitude of the control exocytotic response (134 ± 25 versus 193 ± 29 pC; n = 4). This difference is probably caused by changes in the $[Ca^{2+}]_c$ levels, because total $[Ca^{2+}]_c$ influx was lower in the presence of catestatin, and the kinetics of exocytosis were very similar. In fact, normalized data shown in Figure 9*C* (*right*) indicate that the kinetic curves of the secretory responses elicited by ACh, in the absence or presence of catestatin, were almost superimposed; both curves fitted well to a double exponential, with similar time constants.

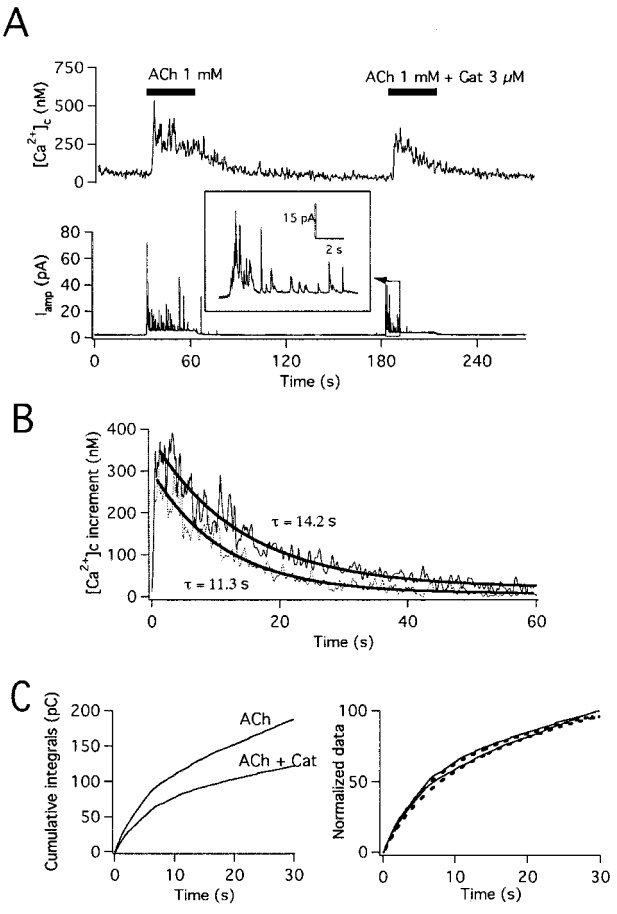

Figure 9. Comparison between $[Ca^{2+}]_c$ signals and catecholamine secretion in single chromaffin cells stimulated with long ACh pulses, in the absence or presence of catestatin. *A*, $[Ca^{2+}]_c$ and electrochemical signals elicited by two sequential ACh pulses (30 sec), separated by a 2 min interval, applied to the same cell. Catestatin was introduced simultaneously to ACh during the second pulse. The *inset* shows the pattern of the secretory signal obtained in the presence of catestatin, at an expanded scale. Amperometric currents consisted of a first rapid phase followed by a second slow-rate secretion where individual spikes could be distinguished easily. *B*, Average of $[Ca^{2+}]_c$ decay obtained from four chromaffin cells stimulated as described above. *Top* and *bottom* traces show the decay of the $[Ca^{2+}]_c$ signal after the ACh application, in the absence or presence of the peptide, respectively. Curves could be fitted to single exponential, giving the control time constants (τ) shown in the figure. *C*, *Left panel*, The cumulative integrals of spikes obtained from ACh-treated or ACh + catestatin (*ACh + Cat*)-treated cells. After integration of individual responses, the average curve was obtained from four cells stimulated with pulses of ACh and ACh + catestatin. *Right panel* shows the normalized data for kinetic comparisons. Each curve was fitted to a double exponential.

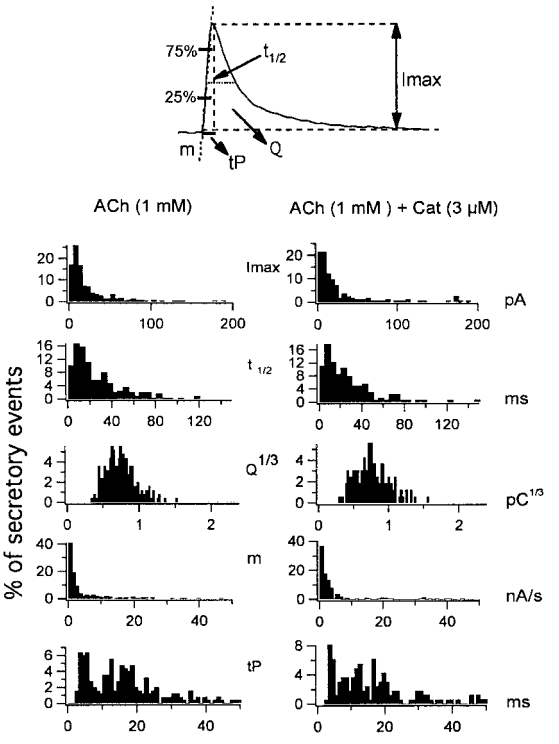

Figure 10. Effect of catestatin on the characteristics of single fusion events. Frequency histograms were obtained during analysis of individual amperometric spikes obtained in cells stimulated with ACh (30 sec), in the absence (*left*) or presence (*right*) of catestatin. On the *top*, an example of a typical spike indicates the parameters measured. These parameters include the peak amplitude (I_{max}), half-width ($t_{1/2}$; duration of the amperometric signal at 50% of its peak amplitude), cubic root of quantal charge ($Q^{1/3}$; considering quantal charge as the time integral of individual amperometric spikes), ascending slope (*m*; calculated from the linear part of the trace located between 25 and 75% of the I_{max}), and time-to-peak (*tP*; determined between the point at which the back-extrapolation of the slope line crossed the base line at the point of I_{max}). Data are pooled from 250 (control) or 163 (catestatin) individual secretory spikes.

The membrane fusion stages of exocytosis were not affected by catestatin

Detailed analysis of individual amperometric spikes elicited by ACh pulses (1 mM, 30 sec) applied to chromaffin cells, in the absence or presence of catestatin, is a good approach for studying whether catestatin could affect the last step of exocytosis, consisting of the fusion of the vesicle with the plasma membrane, forming an exocytotic fusion pore with release of catecholamines and other granule contents (including catestatin) from the vesicle matrix (Alvarez de Toledo et al., 1993). Figure 10 shows the frequency histograms of the peak amplitudes (I_{max}), the half-width ($t_{1/2}$ = duration of the amperometric signal at 50% of its peak amplitude), cubic root of quantal charge ($Q^{1/3}$; considering quantal charge as the time integral of individual amperometric spikes), ascending slope (*m*) and time-to-peak (*tP*), both in control conditions (*left*) or in the presence of catestatin (*right*). Results indicate that the mean charge value for ACh (0.48 pC ± 0.02; $n = 250$) was similar to that obtained in the presence of catestatin (0.55 ± 0.04 pC; $n = 163$). The other kinetic parameters also remained unaltered when ACh versus ACh plus catestatin were compared: $t_{1/2}$ = 19.9 ± 6.1 msec versus 24.6 ± 1.9 msec; I_{max} = 22.8 ± 1.8 pA versus 28.7 ± 3.2 pA; m = 5.2 ± 0.6 nA/sec versus 7.6 ± 0.1 nA/sec; and tP = 22.5 ± 1.5 msec versus 25.2 ± 2.7 msec. Furthermore, no significant differences were found in the occurrence of the foot signals (reflecting transmitter leakage through an early fusion pore that does not dilate immediately) of the amperometric events in the presence of catestatin (9.2%) with respect to control (10.8%).

DISCUSSION

Using several combinations of neuronal nAChR subunits expressed in oocytes, we performed the first electrophysiological study on the interaction between catestatin and the nicotinic receptor. Our data indicate that catestatin is a potent and reversible blocker of the receptor, without significant discrimination among different nAChR subtypes tested. Moreover, in this paper

we present the first detailed analysis, at the single chromaffin cell level, of how catestatin affects the kinetics and different stages of the exocytotic process.

The characteristics of catestatin inhibition on I_{ACh} through $\alpha_3\beta_4$ nAChRs are compatible with a noncompetitive mechanism, as documented previously in PC12 cells (Mahata et al., 1997). Molecules known to act as noncompetitive blockers on muscle, electric organ, and neuronal nicotinic receptors might inhibit ion translocation on interacting with two main categories of sites topographically distinct from the ACh-binding sites: (first) a high affinity site located within the ion channel pore where the blockers sterically hinder ion flux, and (second) multiple low-affinity sites, located at the interface of the receptor with the membrane lipids (Léna and Changeux, 1993; Galzi and Changeux, 1995). Also, a third possibility exists that noncompetitive blockers may physically occlude the channel at the extracellular mouth, outside of the potential field of the membrane.

The following findings are compatible with the hypothesis that catestatin might be entering and occluding the nAChR channel by a mechanism compatible with an open channel blockade. (1) The EC_{50} for ACh became smaller rather than larger in the presence of catestatin (66 vs 94.7 μM); (2) the effectiveness of the peptide on I_{ACh} is greater at higher agonist concentrations (Fig. 2*B*); (3) the strong voltage-dependence of blockade (Fig. 3) and (4) the more frequently the receptors are activated, the greater the degree of blockade produced (Fig. 4*C*). At this moment, how catestatin is accommodated within the nAChR channel is a matter of speculation, although on the basis of its predicted three-dimensional structure, we have proposed a model for the catestatin docking on the *Torpedo* nicotinic receptor channel (Tsigelny et al., 1998). Molecular modeling of the catestatin region reveals a β-strand/loop/β-strand structure secured by hydrophobic interactions, the longitudinal axis of which, at 25 Å, is likely to occlude the nicotinic cation pore at the pore vestibule. If this is also true for the neuronal $\alpha_3\beta_4$ nAChR, and the electropositive loop structure of catestatin (with three directionally displayed positive arginine side chains) entered the channel deeply enough, then the inhibition of I_{ACh} by the peptide should be sensitive to the potential across the membrane. This is indeed the case, according to the results shown in Figure 3.

Additionally, a striking finding is that the preincubation with catestatin produces a greater inhibition of the peak I_{ACh} responses than simple coapplication of the peptide with agonist (Fig. 1*C* and *inset*). These different degrees of blockade could be interpreted in various ways. One possibility is that catestatin, as occurs with many other use-dependent inhibitors, has an increased effect with pre-equilibration because it is present at its effective concentration all during the activation phase of the agonist-evoked response. Because solution exchange is relatively slow in oocyte experiments, during a coapplication-evoked response there is a phase shortly before the peak I_{ACh} when channels are opening in the presence of a relatively low concentration of antagonist. If this hypothesis is true, much of the preincubation effect of catestatin on peak I_{ACh} (IC_{50} values = 4.9 and 0.4 μM, in the absence or presence of preincubation; data obtained from Fig. 1*C*) would disappear if the concentration–response curves for the peptide were calculated in regard to net charge of current rather than the peak amplitude. However, our results indicated that this is not the case, because the differences in blockade between the two modes of catestatin application were still preserved when IC_{50} values were referred to net charge (2.1 and 0.2 μM, in the absence or presence of preincubation, respectively). The other possibility is that during the preincubation period catestatin could bind to a second site located outside the channel. This second site could correspond to the low-affinity binding sites for the noncompetitive antagonists (Léna and Changeux, 1993; Galzi and Changeux, 1995). After binding to high- and low-affinity binding sites, catestatin (like most of the noncompetitive blockers) might increase the affinity of the receptor for nicotinic ligands, a phenomenon that may occur in the absence of agonist and possibly result from the stabilization of the desensitized state of the receptor (Heidmann and Changeux, 1979a,b; Boyd and Cohen, 1984).

Our results do not provide precise data about the comparative potency of the peptide on the four nAChR subunit combinations assayed, because we have not used equally effective ACh concentrations to construct the catestatin concentration–response curves (Fig. 5*B*). Nevertheless, because the only concentration of ACh used to build these curves (100 μM) matches with the EC_{50} values of ACh acting on $\alpha_3\beta_4$ and α_7 nAChRs (98 and 95 μM, respectively), and similar IC_{50} values for catestatin blockade on both receptor types were found, it is possible to conclude that the two main classes of nAChRs controlling the catecholamine release at the splanchnic–chromaffin cell synapse (López et al., 1998) are potential targets for catestatin. Moreover, the fact that the rest of the nAChR subtypes tested do not differ significantly in their sensitivity to the peptide suggests that catestatin might be a ubiquitous regulator of the cholinergic neurotransmission in other areas in addition to the adrenal medulla, i.e., the brain, where α_4 and β_2 nAChR subunits predominate (Gopalakrishnan et al., 1996), or sympathetic ganglia that express α_3, β_2, α_7, and β_4 nAChR subunits (Yu and Role, 1998; Xu et al., 1999) and where endogenously formed catestatin has been documented (Taylor et al., 2000).

The ability of catestatin to interact with the two classes of nAChRs expressed by chromaffin cells (present results), the existence of the peptide *in vivo* [Taylor et al. (2000); present results shown in Fig. 6], and its release by an exocytotic mechanism from stimulated chromaffin cells (Taylor et al., 2000), as well as its effects in various animal species and catecholaminergic cell types (Mahata et al., 1997; present results), all support the idea that this peptide is the first-described endogenous component of chromaffin granules able to modulate the secretory response at the first step of the physiological exocytotic process, the nicotinic receptor. This is substantially different from other known endogenous components of the chromaffin granules (i.e., ATP and enkephalins), which regulate the exocytotic response by a more indirect mechanism by modulating the voltage-dependent Ca^{2+} channel activity (Albillos et al., 1996).

Could catestatin directly affect the exocytotic process independently of its action on the receptor? Our results indicate that this is not the case, because the peptide inhibits ACh-evoked secretion through the reduction of Ca^{2+} influx without influencing the efficacy of $[Ca^{2+}]_c$ increments to trigger the exocytotic process in single chromaffin cells (Fig. 8). An interesting finding is that for brief ACh pulses (5 sec), catestatin needed to be preincubated to obtain a clear and significant effect on the $[Ca^{2+}]_c$ signal and the amperometric current (Fig. 7). This finding might be interpreted according to the mechanisms of interaction between the peptide and the $\alpha_3\beta_4$ nAChR proposed previously. Thus, in the absence of preincubation, the peptide is not bound to the external site of the channel, and its ability to penetrate into the open channel, blocking secretion, is limited by the brief ACh exposure. However, when longer ACh stimulation periods are used (30 sec), catestatin had sufficient time to interact with both binding sites,

reducing significantly both the $[Ca^{2+}]_c$ and the amperometric current (Fig. 9).

Analysis of the secretory pattern elicited by ACh (30 sec) revealed an initial rapid phase, followed by a second slow-rate secretion phase (Fig. 9*A*). This kinetic pattern is similar to that obtained after continuous depolarization of single bovine chromaffin cells with a high $[K^+]$ solution (Gil et al., 1998; Alés et al., 2000). Although the first phase most likely reflects fusion and release of readily releasable vesicles that require only an elevation of $[Ca^{2+}]_c$ for exocytosis (Thomas et al., 1993; Xu et al., 1998), the second phase probably represents vesicles that need lower $[Ca^{2+}]_c$ levels to undergo priming and maturation before they are ready for fusion (Xu et al., 1998). Although the total amount of catecholamines secreted in the presence of catestatin was significantly reduced, the kinetics of the secretory process were not affected (Fig. 9*C*). The finding that catestatin increases the rate of $[Ca^{2+}]_c$ decay (Fig. 9*B*) most likely implies that basal $[Ca^{2+}]_c$ levels could be recovered faster in the presence of the peptide, allowing cells to be quickly prepared to initiate a new round of exocytosis after the arrival of a new stimulus. We have not found that catestatin prevents receptor desensitization, previously documented by Mahata et al. (1999). This is most likely because of large experimental differences in the exposure period to the agonist, a few seconds in the present paper versus 10 min in previous studies, which in our studies completely desensitized all of the ACh-evoked responses.

Catecholamine secretion from chromaffin cells occurs through a process involving docking, fusion, and incorporation of the vesicle membrane into the cytoplasmic membrane; then, the matrix vesicle core is exposed to the extracellular fluid. The time course of the late step of exocytosis might be altered by a different mechanism, including modification of the affinity of catecholamines for the intragranular matrix (Schroeder et al., 1996). In this case, chromogranin A, ATP, and Ca^{2+} have been implicated in the intragranular Donnan complex of catecholamines (Kopell and Westhead, 1982; Sen and Sharp, 1982; Helle et al., 1990), and therefore, slight modifications in the conformation of chromogranin A might account for large changes in its affinity for catecholamines, with consequent changes in release (Leszczyszyn et al., 1990; Schroeder et al., 1996, Rahamimoff and Fernández, 1997). Then, the possibility existed that fragmentation of chromogranin A to catestatin might modify catecholamine release by altering the last step of the exocytotic process. Our results indicate that this is not the case, because the peptide did not modify the quantal size and pattern of the vesicle release (Fig. 10).

In conclusion, the catestatin fragment of chromogranin A exerts its autocrine modulatory role on catecholamine secretion by a direct interaction with the nicotinic receptor itself, reducing Na^+ and Ca^{2+} influx into the cell, without affecting the kinetics or the last step of the exocytotic process. The fact that the modulatory mechanism of catestatin on the nAChR displays a more pronounced inhibitory effect during prolonged and stronger ACh pulses might have physiological relevance. Thus, the endogenous peptide could exert a major control at the higher frequencies of splanchnic nerve stimulation (i.e., extremely stressful situations), in which a more effective modulatory action might be advantageous in avoiding the negative consequences of an excessive release of catecholamines to the bloodstream.

REFERENCES

Aardal S, Helle KB (1992) The vasoinhibitory activity of bovine chromogranin A fragment (vasostatin) and its independence of extracellular calcium in isolated segments of human blood vessels. Regul Pept 41:9–19.

Albillos A, Carbone E, Gandía L, García AG, Pollo A (1996) Opioid inhibition of Ca^{2+} channels subtypes in bovine chromaffin cells: selectivity of action and voltage-dependence. Eur J Neurosci 8:1561–1570.

Alés E, Gabilán NH, Cano-Abad MF, García AG, López MG (2000) The sea anemone toxin bc2 induces continuous or transient exocytosis, in the presence of sustained levels of high Ca^{2+} in chromaffin cells. J Biol Chem 275:37488–37495.

Almers W, Neher E (1985) The Ca^{2+} signal from fura-2 loaded mast cells depends strongly on the method of dye-loading. FEBS Lett 92:13–18.

Alvarez de Toledo G, Fernández-Chacon R, Fernández JM (1993) Release of secretory products during transient vesicle fusion. Nature 363:554–558.

Blaschko H, Comline RS, Schneider FH, Silver M, Smith AD (1967) Secretion of a chromaffin granule protein, chromogranin, from the adrenal gland after splanchnic stimulation. Nature 215:58–59.

Boyd ND, Cohen JB (1984) Desensitization of membrane-bound *Torpedo* acetylcholine receptor by amine noncompetitive antagonists and alcohol: studies of (^{3}H)acetylcholine binding and $^{22}Na^+$ ion fluxes. Biochemistry 23:4023–4033.

Campos-Caro A, Smillie FI, Domínguez Del Toro E, Rovira JC, Vicente-Agulló F, Chapuli J, Juíz JM, Sala S, Sala F, Ballesta JJ, Criado M (1997) Neuronal nicotinic acetylcholine receptor on bovine chromaffin cells: cloning, expression and genomic organization of receptor subunits. J Neurochem 68:488–497.

Chow RH, Von Rüden L, Neher E (1992) Delay in vesicle fusion revealed by electrochemical monitoring of single secretory events in adrenal chromaffin cells. Nature 356:60–63.

Criado M, Alamo L, Navarro A (1992) Primary structure of an agonist binding subunit of the nicotinic acetylcholine receptor from bovine adrenal chromaffin cells. Neurochem Res 17:281–287.

Galzi JL, Changeux JP (1995) Neuronal nicotinic receptors: molecular organization and regulations. Neuropharmacology 34:563–582.

Gandía L, García AG, Morad M (1993) ATP modulation of calcium channels in chromaffin cells. J Physiol (Lond) 244:253–262.

García-Guzman BM, Sala F, Sala S, Campos-Caro A, Stühmer W, Gutiérrez LM, Criado M (1995) α-Bungarotoxin-sensitive nicotinic receptors on bovine chromaffin cells: molecular cloning, functional expression and alternative splicing of the α_7 subunit. Eur J Neurosci 7:647–655.

Gil A, Viniegra S, Gutierrez LM (1998) Dual effects of botulinum neurotoxin A on the secretory stages of chromaffin cells. Eur J Neurosci 10:3369–3378.

Gopalakrishnan M, Monteggia LM, Anderson DJ, Molinari EJ, Piattoni-Kaplan M, Donnelly-Roberts D, Arneric SP, Sullivan JP (1996) Stable expression, pharmacological properties and regulation of the human neuronal nicotinic acetylcholine alpha 4 beta 2 receptor. J Pharmacol Exp Ther 276:289–297.

Goumon Y, Strub JM, Moniatte M, Nullans G, Poteur L, Hubert P, Van Dorsselaer A, Aunis D, Metz-Boutigue MH (1996) The C-terminal bisphosphorylated proenkephalin-A-(209–237)-peptide from adrenal medullary chromaffin granules possesses antibacterial activity. Eur J Biochem 235:516–525.

Grynkiewicz G, Poenie M, Tsien RY (1985) A new generation of Ca^{2+} indicators with greatly improved fluorescence properties. J Biol Chem 260:3440–3450.

Heidmann T, Changeux JP (1979a) Fast kinetic studies on the interaction of a fluorescent agonist with the membrane-bound acetylcholine receptor from *T. marmorata*. Eur J Biochem 94:255–279.

Heidmann T, Changeux JP (1979b) Fast kinetic studies on the allosteric interactions between acetylcholine receptor and local anesthetic binding sites. Eur J Biochem 94:281–296.

Helle KB, Reed RK, Ehrhart M, Aunis D, Angeletti RH (1990) Chromogranin A: osmotically active fragments and their susceptibility to proteolysis during lysis of the bovine chromaffin granules. Acta Physiol Scand 138:565–547.

Hernández-Guijo JM, De Pascual R, García AG, Gandía L (1998) Separation of calcium channel current components in mouse chromaffin cells superfused with low- and high-barium solutions. Pflügers Arch 436:75–82.

Herrero CJ, García-Palomero E, Pintado AJ, García AG, Montiel C (1999) Differential blockade of rat $\alpha_3\beta_4$ and α_7 neuronal nicotinic receptors by ω-conotoxin MVIIC, ω-conotoxin GVIA and diltiazem. Br J Pharmacol 127:1375–1387.

Huttner WB, Gerdes HH, Rosa P (1991) Chromogranins/secretogranins—widespread constituents of secretory granule matrix in the endocrine cells and neurons. In: Markers for neural and endocrine cells (Gratzl M, Langley K), pp 93–131. Weinheim, Germany: VCH Verlagsgesellsschaft.

Kilpatrick DL, Slepetis R, Kirshner N (1981) Ion channels and membrane potential in stimulus-secretion coupling in adrenal medulla cells. J Neurochem 36:1245–1255.

Kopell WN, Westhead EW (1982) Osmotic pressures of solutions of

ATP and catecholamines relating to storage in chromaffin granules. J Biol Chem 257:5707–5710.
Kumakura K, Karoun F, Guidotti A, Costa E (1980) Modulation of nicotinic receptors by opiate receptor agonists in cultured adrenal chromaffin cells. Nature 283:489–492.
Léna C, Changeux JP (1993) Allosteric modulations of the nicotinic acetylcholine receptor. Trends Neurosci 16:181–186.
Leszczyszyn DJ, Jankowski JA, Viveros OH, Diliberto EJ, Near JA, Wigthman RM (1990) Nicotinic receptor-mediated catecholamine secretion from individual chromaffin cells. Chemical evidence for exocytosis. J Biol Chem 265:14736–14737.
López MG, Montiel C, Herrero CJ, García-Palomero E, Mayorgas I, Hernández-Guijo JM, Villarroya M, Olivares R, Gandía L, Mcintosh JM, Olivera BM, García AG (1998) Unmasking the functions of the chromaffin cell α_7 nicotinic receptor by using short pulses of acetylcholine and novel selective blockers. Proc Natl Acad Sci USA 95:14184–14189.
Mahata SK, O'Connor DT, Mahata M, Yoo SH, Taupenot TL, Wu H, Gill BM, Parmer RJ (1997) Novel autocrine feedback control of catecholamine release: a discrete chromogranin A fragment is a noncompetitive nicotinic cholinergic antagonist. J Clin Invest 100:1623–1633.
Mahata SK, Mahata M, Parmer RJ, O'Connor DT (1999) Desensitization of catecholamine release. The novel catecholamine release-inhibitory peptide catestatin (chromogranin A344–364) acts at the receptor to prevent nicotinic cholinergic tolerance. J Biol Chem 274:2920–2928.
Mahata SK, Mahata M, Wakade AR, O'Connor DT (2000) Primary structure and function of the catecholamine release inhibitory peptide catestatin (chromogranin $A_{344-364}$): identification of amino acid residues crucial for activity. Mol Endocrinol 14:1525–1535.
Miledi R, Parker I (1984) Chloride current induced by injection of calcium into *Xenopus* oocytes. J Physiol (Lond) 357:173–183.
Miledi R, Parker I, Sumikawa K (1989) Properties of acetylcholine receptors translated by cat muscle mRNA in *Xenopus* oocytes. EMBO J 1:1307–1312.
Montiel C, Herrero CJ, García-Palomero E, Renart J, García AG, Lomax RB (1997) Serotonergic effects of dotarizine in coronary artery and in oocytes expressing 5-HT_2 receptors. Eur J Pharmacol 332:183–193.
Papke RL, Thinschmidt JS (1998) The correction of alpha7 nicotinic acetylcholine receptor concentration-response relationships in *Xenopus* oocytes. Neurosci Lett 256:163–166.
Pintado AJ, Herrero CJ, García AG, Montiel C (2000) The novel Na^+/Ca^{2+} exchange inhibitor KB-R7943 also blocks native and expressed neuronal nicotinic receptors. Br J Pharmacol 130:1893–1902.
Rahamimoff R, Fernández JM (1997) Pre- and postfusion regulation of transmitter release. Neuron 18:17–27.
Schroeder TJ, Borges R, Finnegan JM, Pihel K, Amatore C, Wightman RM (1996) Temporally resolved, independent stages of individual exocytotic secretion events. Biophys J 70:1061–1068.
Seguela P, Wadiche J, Dineley-Miller K, Dani JA, Patrick JW (1993) Molecular cloning, functional expression and distribution of rat brain α_7: a nicotinic cation channel highly permeable to calcium. J Neurochem 13:596–604.
Segura F, Brioso MA, Gómez JF, Machado D, Borges R (2000) Automatic analysis for amperometrical recordings of exocytosis. J Neurosci Methods 103:151–156.
Sen R, Sharp R (1982) Molecular mobilities and the lowered osmolality of the chromaffin granule aqueous phase. Biochim Biophys Acta 721:70–82.
Stafford GA, Oswald RE, Weiland GA (1994) The beta subunit of neuronal nicotinic acetylcholine receptors is a determinant of the affinity for substance P inhibition. Mol Pharmacol 45:758–762.
Strub JM, Goumon Y, Lugardon K, Capon C, Lopez M, Moniatte M, Van Dorsselaer A, Aunis D, Metz-Boutigue MH (1996) Antibacterial activity of glycosylated and phosphorylated chromogranin A-derived peptide 173–194 from bovine adrenal medullary chromaffin granules. J Biol Chem 271:28533–28540.
Tatemoto K, Efendic S, Mutt V, Makk G, Feistner GJ, Barchas JD (1986) Pancreastatin, a novel pancreatic peptide that inhibits insulin secretion. Nature 324:476–478.
Taylor CV, Taupenot L, Mahata SK, Mahata M, Wu H, Yasothornsrikul S, Toneff T, Caporale C, Jiang Q, Parmer RJ, Hook VY, O'Connor DT (2000) Formation of the catecholamine release-inhibitory peptide catestatin from chromogranin A. Determination of proteolytic cleavage sites in hormone storage granules. J Biol Chem 275:22905–22915.
Thomas P, Wong JG, Lee AK, Almers W (1993) A low affinity Ca^{2+} receptor controls the final steps in peptide secretion from pituitary melanotrophs. Neuron 11:93–104.
Trifaró JM, Lee RW (1980) Morphological characteristics and stimulus-secretion coupling in bovine adrenal chromaffin cell cultures. Neuroscience 5:1533–1546.
Tsigelny I, Mahata SK, Taupenot L, Preece NE, Mahata M, Khan I, Parmer RJ, O'Connor DT (1998) Mechanism of action of chromogranin A on catecholamine release: molecular modeling of the catestatin region reveals a beta-strand/loop/beta-strand structure secured by hydrophobic interactions and predictive of activity. Regul Pept 77:43–53.
Wilson SP, Kirshner N (1977) The acetylcholine receptor of the adrenal medulla. J Neurochem 28:687–695.
Winkler H, Apps DK, Fischer-Colbrie R (1986) The molecular function of adrenal chromaffin granules: established facts and unresolved topics. Neuroscience 18:261–290.
Xu T, Binz T, Niemann H, Neher E (1998) Multiple kinetic components of exocytosis distinguished by neurotoxin sensitivity. Nat Neurosci 1:192–200.
Xu W, Orr-Urtreger A, Nigro F, Gelber S, Sutcliffe CB, Armstrong D, Patrick JW, Role LW, Beaudet AL, De Biasi M (1999) Multiorgan autonomic dysfunction in mice lacking the $\beta 2$ and the $\beta 4$ subunits of neuronal nicotinic acetylcholine receptors. J Neurosci 19:9298–9305.
Yu CR, Role LW (1998) Functional contribution of the alpha7 subunit to multiple subtypes of nicotinic receptors in embryonic chick sympathetic neurones. J Physiol (Lond) 15:651–665.